A&A 632, L9 (2019)
https://doi.org/10.1051/0004-6361/201936942
© F. Kiefer 2019

Astronomy & Astrophysics

LETTER TO THE EDITOR

Determining the mass of the planetary candidate HD 114762 b using *Gaia*

Flavien Kiefer

Sorbonne Université, CNRS, UMR 7095, Institut d'Astrophysique de Paris, 98 bis bd Arago, 75014 Paris, France
e-mail: flavien.kiefer@iap.fr

Received 16 October 2019 / Accepted 13 November 2019

ABSTRACT

The first planetary candidate discovered by Latham et al. (1989, Nature, 339, 38) with radial velocities around a solar-like star other than the Sun, HD 114762 b, was detected with a minimum mass of 11 M_J. The small $v \sin i \sim 0\,\mathrm{km\,s^{-1}}$ that is otherwise measured by spectral analysis indicated that this companion of a late-F subgiant star better corresponds to a massive brown dwarf (BD) or even a low-mass M-dwarf seen nearly face-on. To our knowledge, the nature of HD 114762 b is still undetermined. The astrometric noise measured for this system in the first data release, DR1, of the *Gaia* mission allows us to derive new constraints on the astrometric motion of HD 114762 and on the mass of its companion. We use the method GASTON, introduced in a preceding paper, which can simulate *Gaia* data and determine the distribution of inclinations that are compatible with the astrometric excess noise. With an inclination of $6.2^{+1.9}_{-1.3}$ degree, the mass of the companion is constrained to $M_b = 108^{+31}_{-26}\,M_J$. HD 114762 b thus indeed belongs to the M-dwarf domain, down to brown dwarfs, with $M_b > 13.5\,M_J$ at the 3σ level, and is not a planet.

Key words. stars: individual: HD 114762 – planetary systems – stars: low-mass – astrometry

1. Introduction

The HD 114762 system was discovered by Latham et al. (1989) to host a possible brown dwarf or giant planet with a period of 84 days and a minimum mass of 11 M_J. This planetary mass companion was later confirmed by Cochran et al. (1991) and subsequent monitoring (Butler et al. 2006; Kane et al. 2011). Not long after its discovery, however, it was found that the hosting star, a very metal-poor late-F subgiant, had a remarkably small $v \sin i \sim 0 - 1.5\,\mathrm{km\,s^{-1}}$ compared to its expected rotational speed $v_{\rm rot} \sim 8\,\mathrm{km\,s^{-1}}$ (Cochran et al. 1991; Hale 1995). This implied a far from edge-on inclination, which led to a reconsideration of the companion mass as lying beyond the planetary mass regime (>20 M_J) and within the brown dwarf mass-domain. Nonetheless, it was suggested that the considerable age (>10 Gyr) and low metallicity (−0.7 dex) of the F9 primary could imply smaller stellar rotational speed, down to $2\,\mathrm{km\,s^{-1}}$ and thus a higher inclination of the HD 114762 b orbit (Mazeh et al. 1996).

Moreover, non-zero spin-orbit misalignment of exoplanet orbits and stellar spin has been measured today for many transiting systems (e.g., Winn et al. 2005; Hébrard et al. 2008; Triaud et al. 2010; Johnson et al. 2017). This considerably weakens the outcome of measuring a discrepancy between stellar rotation rates and $v \sin i$ on inferring an orbital inclination. The discovery of a visual binary companion, HD 114762 B, at a separation of 130 au, implied that the obliquity angle of the planetary orbit could indeed be misaligned with the stellar rotation axis by dynamical effects, such as Lidov-Kozai mechanisms (Patience et al. 2002; Bowler et al. 2009).

On the other hand, with a mass as high as 11 M_J and a stellar metallicity of −0.7 dex, HD 114762 b stands apart from the massive exoplanet population. The stellar metallicity for a planet mass beyond 1 M_J hardly reaches levels as low as −0.5 dex (Matsuo et al. 2007). Core-collapse can well explain the distribution of massive exoplanets above a metallicity of −0.5 dex, but fails to explain high-mass companions around low-metallicity stars such as HD 114762 b (Mordasini et al. 2012).

Finally, the possibility of transits of HD 114762 b was rejected, which excluded an edge-on configuration (Kane et al. 2011). The nature of the companion to HD 114762 remains unknown, and to our knowledge, no clear conclusion on its mass has been reached.

The final release of the *Gaia* mission (Gaia Collaboration 2016b), based on an astrometry of an extreme precision, is forseen to allow determining the exact mass of many systems that are detected with radial velocities (RV; Perryman et al. 2014). Kiefer et al. (2019, hereafter K19), showed that even at the level of the astrometric noise recorded in the first data release (DR1) of the *Gaia* mission, the powerful precision of *Gaia* has been able to provide strong constraints on the mass of companions that are detected with RV. In particular, the masses of a few brown dwarf (BD) candidates were constrained to rather be in the M-dwarf mass regime, while some were confirmed to have a BD mass.

Applying the analysis and methods developed in K19, called GASTON, to the case of HD 114762, we here add new constraints on the inclination of the orbit and mass of its companion. This is based on DR1 of the *Gaia* mission (Gaia Collaboration 2016a).

Section 2 summarizes the main properties of the HD 114762 A system. Section 3 presents the astrometric measurements obtained by *Gaia* in the DR1 and the derived inclination and

Open Access article, published by EDP Sciences, under the terms of the Creative Commons Attribution License (https://creativecommons.org/licenses/by/4.0), which permits unrestricted use, distribution, and reproduction in any medium, provided the original work is properly cited.

Table 1. Stellar properties of HD 114762 A.

Parameters	Values
RA [a]	13:12:19.7467
Dec [a]	+17:31:01.6114
V [a]	7.3
$B-V$ [a]	0.525
π [mas] [b]	25.88 ± 0.46
Distance [pc] [b]	38.64 ± 0.69
Spectral type [c]	F9
$T_{\rm eff}$ [K] [c]	5869 ± 13
$\log g$ [s.i.] [c]	4.18 ± 0.03
[Fe/H] [dex] [a]	$-0.72^{+0.05}_{-0.07}$
Age [Gyr] [e]	12 ± 4
$M_\star$ [$M_\odot$] [c]	0.80 ± 0.06
$v \sin i$ [km s^{-1}] [d]	1.77 ± 0.50
$v_{\rm rot}$ [km s^{-1}] [e]	8.3 ± 2.2
$I_\star$ [°] [f]	13.5 ± 5

Notes. [a]From SIMBAD. [b]From *Gaia* DR1, accounting for the average HIPPARCOS-*Tycho* position of the target at $T_{\rm ref} = 1991.5$. [c]From Stassun et al. (2017). [d]From Kane et al. (2011). [e]From Nordström et al. (2004). [f]Obtained by Monte Carlo simulations, with $I_c = \arcsin(v \sin i / v_{\rm rot})$ and assuming Gaussian distributions for $v \sin i$ and $v_{\rm rot}$.

mass of the companion of HD 114762 A. In Sect. 4 we discuss the possibility that a wide binary companion might pollute the *Gaia* astrometry of the HD 114762 system. In Sect. 5 we compare the proper motions of the HD 114762 system observed by HIPPARCOS and *Gaia* and discuss them in regard to the existence of several companions. We conclude in Sect. 6.

2. Properties of the HD 114762 A system

Table 1 summarizes the main stellar properties of HD 114762 A. This sub-giant F9 star is located at 40 pc from the Sun, with a parallax of $\pi = 26$ mas and a 7.3 apparent magnitude in the V-band.

Radial velocity data have been collected along the years since the discovery of the low-mass companion of this source. The best radial velocity solution is given in Kane et al. (2011). This is based on Lick observatory spectra collected on a time line of 19 years. An 84-day orbit leads to a robust Keplerian fit of the star reflex motion. The fitted Keplerian as reported in Kane et al. (2011) and corrected with the last stellar mass derivation by Stassun et al. (2017) is given in Table 2. A possible linear trend of 3.5 m s^{-1} yr^{-1}, indicative of an exterior companion, was reported by Kane et al. (2011), but this led to an insignificant improvement of the fit of the RV data. No other supplementary signal was reported in the RV O-C residuals of this star beyond a semi-amplitude of 27 m s^{-1}.

According to the RV solution and the relatively large parallax of this system, the minimum semi-major axis of the orbital motion of the star should be larger than 0.11 mas. With a typical measurement error on the order of 0.5 mas, and at least 180 astrometric measurements, *Gaia* should be able to detect the astrometric motion of the unresolved HD 114762 system, even in the most unfavourable edge-on case.

3. Astrometry of HD 114762 with *Gaia*

Using the GASTON method developed in K19, we used *Gaia* astrometry to constrain the mass of the companion to

Table 2. Kane et al. (2011) Keplerian solution of HD 114762 b, accounting for the newly derived stellar mass by Stassun et al. (2017).

Parameters	Kane et al. (2011)
P [days]	83.9151 ± 0.0030
K [m s^{-1}]	612.48 ± 3.52
e	0.3354 ± 0.0048
ω [°]	201.28 ± 1.01
$T_{\rm p}$	$2\,449\,889.106 \pm 0.186$
$M_{\rm b} \sin i$ [$M_{\rm J}$]	10.69 ± 0.56
$a_{\rm b}$ [AU]	0.363 ± 0.0121
$a_\star \sin i$ [mas] [a]	0.121 ± 0.012

Notes. [a]Calculated as $a_\star \sin i = (M_{\rm b} \sin i / M_\star)\, a_{\rm b}\, \pi\,({\rm mas})$.

HD 114762 A. GASTON uses RV Keplerian solutions and the astrometric excess noise published in the *Gaia* DR1 to constrain the inclination of the orbit of the companion and therefore determine its true mass. The principle of this method is simple. GASTON simulates *Gaia* photocenter measurements along the constrained RV orbit with different orbit inclinations with respect to the plane of the sky. Various inclinations can be tested, each leading to a simulated astrometric excess noise $\epsilon_{\rm simu}$. We then constrain the different possible inclinations by comparing the whole set of $\epsilon_{\rm simu}$ with its actual measurement in DR1, $\epsilon_{\rm DR1}$.

Compared to K19, we here added a few improvements to GASTON. We incorporated a Markov chain Monte Carlo (MCMC) process to explore the full parameter space, which accounts for error bars on the RV Keplerian parameters, and an inclination prior distribution $p(\theta) = \sin\theta\, {\rm d}\theta$. Details on the MCMC implementation can be found in the appendix.

The astrometric excess noise ϵ can be found in DR1 (Gaia Collaboration 2016a) and DR2 (Gaia Collaboration 2018). Although it is based on a shorter time line of astrometric measurements (25 July 2014 – 16 September 2015, or 416 days), we used the value of ϵ that is published in DR1. We found it more reliable than the value in DR2 because of the so-called "DOF-bug" that directly affected the dispersion measurement of the final astrometric solution (Lindegren et al. 2018). The value of ϵ for this system was thus retrieved from the *Gaia* DR1 archives[1].

The astrometric excess noise was obtained by estimating the χ^2 of its along-scan angle residuals around the five-parameter solution, as derived by the *Gaia* reduction software (Lindegren et al. 2012). Parallax and proper motion for this star were calculated by *Gaia* taking into account existing HIPPARCOS and *Tycho*-2 astrometric positions as priors. This led to a 25-year baseline for fitting the stellar motion. This implies that the orbital motion of the star with $P = 84$ days should have a negligible effect on the measurement of these parameters during the 416-day time span of DR1.

The DR1 excess noise may incorporate bad spacecraft attitude modeling, which means that the value of ϵ does not consist of binary motion alone (Lindegren et al. 2012). The amplitude of the attitude and calibration modeling errors within ϵ were estimated from its median value in the primary sample of objects observed with *Gaia* (Lindegren et al. 2016), $\epsilon_{\rm med} = 0.5$ mas. The 90% percentile rises at 0.85 mas. Any value of ϵ above that level likely contains true binary astrometric motion. For HD 114762, *Gaia* DR1 reports an astrometric excess noise of 1.09 mas, which thus reveals significant astrometric motion in this system.

[1] http://gea.esac.esa.int/archive/

Table 3. *Gaia* DR1 data for HD 114762 (see definitions in text).

Parameters	Value
$N_{\rm FoV}$	23
$N_{\rm obs}$	130
$N_{\rm orb}$	4.3
ϵ [mas]	1.09
D_ϵ	252
ΔQ	26.33
Duplicated source	False

The *Gaia* DR1 parameters we used are summarized in Table 3. The table includes ϵ, the astrometric excess noise; D_ϵ, the significance of ϵ given a p-value $p = 1 - e^{-D_\epsilon/2}$ (Lindegren et al. 2012); ΔQ, which measures the discrepancy between extrapolated HIPPARCOS-2 models and *Gaia* actual measurements (a value higher than 100 indicates binarity with a semi-major axis that might be larger than 1 au) (Michalik et al. 2014; Kiefer et al. 2019); $N_{\rm orb}$, the number of HD 114762 b orbits covered by the time span of *Gaia* DR1; $N_{\rm obs}$, the total number of along-scan angle measurements of the HD 114762 system performed by *Gaia*; $N_{\rm FoV}$, the number of field-of-view transits of the source on the CCD detector; and finally, "Duplicated source" indicates whether the detections had duplicates or were mismatched with other sources.

No astrometric motion is detected in the comparison of *Gaia* and HIPPARCOS, with $\Delta Q < 100$. This is expected because the orbital period of the system is shorter than 100 days, while the HIPPARCOS-*Gaia* time span is on the order of 25 years. It also shows that no binary companion is attached to this system with periods on the order of a few dozen to a few hundred years. The insignificant trend reported in Kane et al. (2011) might therefore correspond to a companion on an orbital period that is longer than a few hundred years. This might be compatible with the detected companion at 130 au (Patience et al. 2002), for which the minimum possible orbital period (at $e \sim 1$) is 500 years. We discuss this possibility in Sect. 4 below.

The high value $\epsilon = 1.09$ mas very probably is not an artifact of the *Gaia* reduction. This source was not duplicated and has an optimal visual magnitude in the *Gaia* band of 7.3. We cannot find other diagnostics that would rule out the astrophysical nature of this excess noise. We are aware that some astrometric measurements might be affected by pollution through background stars. This diagnosis is not always even certain, however. A recent example of this uncertainty is the eclipsing system NGTS-10, for which an excess noise of ~2 mas is observed in both DR1 and DR2 (McCormac et al. 2019), while a close star is detected as well. McCormac et al. (2019) suspected an occasional mismatch of NGTS-10 with this star.

A widely separated ($\rho = 130$ au; 3.3″) M-dwarf or brown dwarf companion with a magnitude difference of 7.3 in the K band was detected around HD 114762 A (Patience et al. 2002). The magnitude difference is probably larger in the optical band because HD 114762 B was not detected in *Gaia* DR1 or DR2, therefore we are confident that this visual companion does not have the same effect here. However, it remains possible that part of the astrometric excess noise measured in DR1 for HD 114762 A might be due to its reflex motion caused by HD 114762 B. We explore this issue in more detail in Sect. 4 below.

We conclude that *Gaia* likely caught a significant astrometric binary motion in the system of HD 114762, with a semi-major axis as large as $\epsilon = 1.09$ mas (or 0.04 au). With this estimate of ϵ, along the parameters given in Tables 1–3, we used the method described in K19 to derive a constraint on the orbital inclination of HD 114762 b and on its mass.

Table 4. Results of the mass and inclination determination of HD 114762 b with GASTON.

Parameters	Median	1σ confidence interval
P [days]	83.915	83.912–83.918
$e_{\rm b}$	0.566	0.555–0.578
ω [°]	201.3	200.3–202.3
$\Delta T_{\rm p}$ [JD]	−0.0017	−0.1879–0.1861
$M_{\rm b} \sin i$ [$M_{\rm J}$]	10.72	10.33–11.10
$M_\star$ [$M_\odot$]	0.80	0.76–0.84
π [mas]	25.90	25.45–26.35
f_ϵ [(a)]	1.00	0.90–1.10
$\sigma_{\rm jitter}$ [m s^{-1}] [(a)]	3.06	0.98–5.09
$I_{\rm c}$ [°]	4.87	3.96–5.98
$M_{\rm b}$ [$M_{\rm J}$]	141	113–176
$a_{\rm ph}$ [mas] [(b)]	1.35	1.12–1.63
ΔV [(c)]	8.6	7.6–9.6
$\Delta\mu$ [mas yr^{-1}] [(d)]	1.21	0.60–2.07
Accounting for HD 114762 B		
$I_{\rm c}$ [°]	6.20	4.90–8.10
$M_{\rm b}$ [$M_{\rm J}$]	108	82–139
$a_{\rm ph}$ [mas]	1.07	0.83–1.33
ΔV	9.8	8.6–11.3
$\Delta\mu$ [mas yr^{-1}]	1.00	0.49–1.75

Notes. The final results on $I_{\rm c}$, $M_{\rm b}$, $a_{\rm ph}$, ΔV, and $\Delta\mu$ that account for the presence of HD 114762 B are given at the bottom of the table (see also Sect. 4). [(a)] f_ϵ and $\sigma_{\rm jitter}$ are the scaling factor and RV jitter term for the uncertainties of ϵ^2 and K, as explained in the appendix. [(b)]Photocenter semi-major axis (see K19 for definition). [(c)]The estimated magnitude difference between HD 114762 A and HD 114762 b in the optical band. [(d)]The proper motion amplitude fit on the simulated *Gaia* data.

The results of the GASTON simulations are given in Table 4, and the MCMC posterior distributions of all parameters are presented in Fig. A.1. A simulation of *Gaia* measurements is plotted in Fig. 1 along with the derived $I_{\rm c} - \epsilon_{\rm tot}$ relation for this system. The quantity $\epsilon_{\rm tot}$ encloses the total scatter of astrometric measurements (see Appendix A.3 for the exact definition).

We find that the orbit of HD 114762 b probably is almost face-on, with an inclination of $5 \pm 1°$. The mass is revised to be in the M-dwarf regime with $M_{\rm b} = 141^{+35}_{-28}\,M_{\rm J}$. At 3σ the confidence interval extends to 68–331 $M_{\rm J}$. This fully rejects a planetary mass for this companion. We measure a photocenter semi-major axis of $1.35^{+0.28}_{-0.23}$ mas, and a difference in visual magnitude between the primary and this companion of 8.6 ± 1.0. This leads to a total separation between these components of $a_{\rm tot} = 0.36 \pm 0.11$ au.

4. Binary component HD 114762 B

As reported in Patience et al. (2002), the system of HD 114762 is also a wide visual binary pair A and B. The separation between the two components was measured to be 3.3″, with a magnitude difference in the K band of 7.3 mag. This led to a derived mass of the secondary component of about 0.088 $M_\odot$ (Bowler et al. 2009) and a separation of 130 au. The minimum orbital period of this wide-orbit companion is thus of 600 years if it is on a very eccentric orbit and is detected at apoastron.

It is important to determine whether this companion B, as yet undetected by *Gaia* (probably weaker than magnitude 18

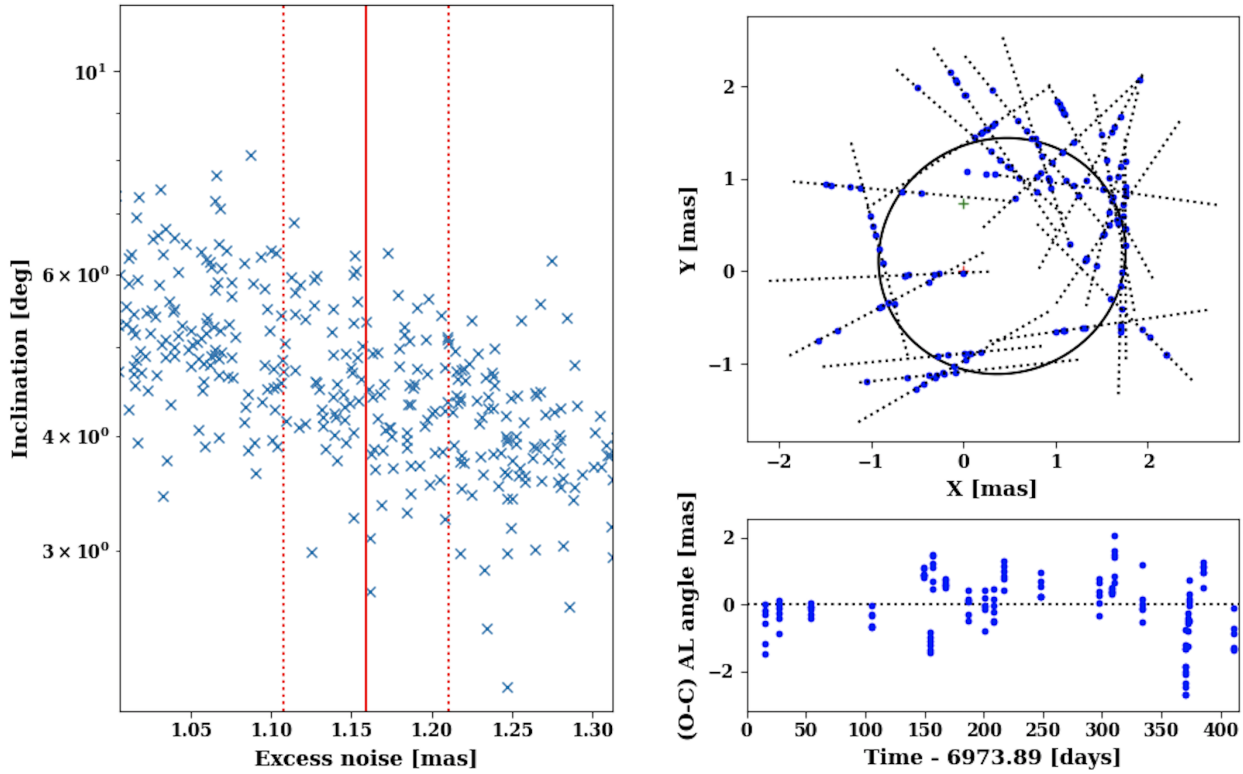

Fig. 1. *Left panel*: simulated excess noise with respect to inclination. The red dash lines indicate the error interval around the total excess noise $\epsilon_{\rm tot}$, as explained in the text and Appendix A.3 (solid red line). *Right panels*: astrometric simulation for the median inclination ($I_{\rm c} = 4.87°$) that is compatible with the *Gaia* data. The black dotted lines show the along-scan angle at each FoV transit; the red plus is the focus of the orbit, and the green plus is the centroid of measurements. The residuals in the *bottom panel* are calculated relative to the centroid.

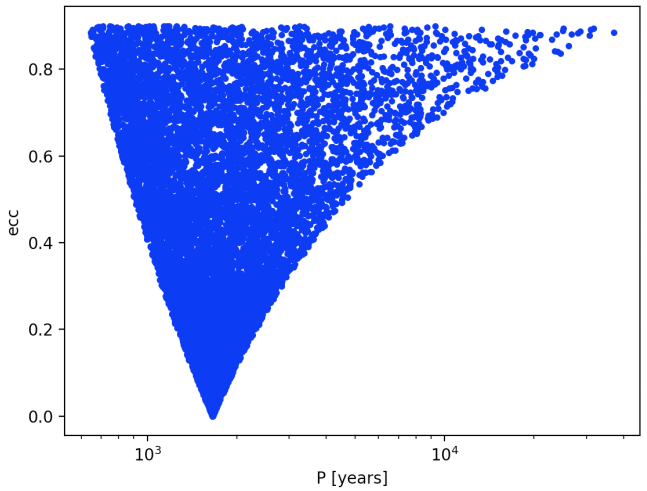

Fig. 2. Eccentricities and periods of the HD 114762 B orbit tested during simulations of *Gaia* measurements of the astrometric motions of HD 114762 A as the result of HD 114762 B alone.

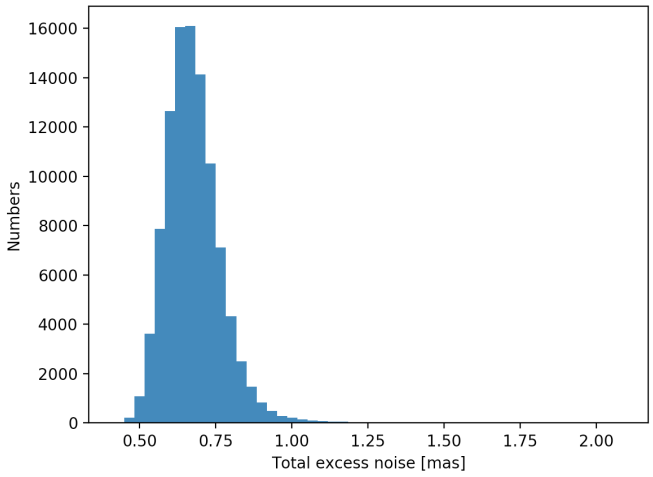

Fig. 3. Distribution of the excess noise simulated for HD 114762 A as the result of HD 114762 B alone.

in the G band) might be at the origin of the astrometric excess noise that was measured by *Gaia* in DR1 for the HD 114762 system. With the same core as used above, we simulated 100 000 different orbital configurations of HD 114762 B and calculated the possible values of the excess noise that would be measured with *Gaia* during the DR1 campaign if they were the result of HD 114762 B alone. We varied the semi-major axis from $\rho/(1-e)$ to $\rho/(1+e)$, with $\rho = 130$ au the separation between components A and B, and e a random eccentricity between 0 and 1. The different periods and eccentricities we tested are plotted in Fig. 2. Random inclinations were drawn from the density function $p(\theta) = \sin\theta\,{\rm d}\theta$. In all cases, the corresponding radial velocity variations on a baseline of 19 years are always smaller than 12 m s^{-1}, which is smaller than the amplitude of the O–C residuals and smaller than a possible linear trend in the data of Kane et al. (2011).

The excess noise of the reflex motion of HD 114762 A as the result of HD 114762 B is typically $\epsilon = 0.55 \pm 0.11$ mas, and 68.3% of the simulations lie within this interval. This is presented in Fig. 3. The value $\epsilon_{\rm DR1} = 1.09$ mas is reached in only 0.14% of the simulations. We can therefore exclude that

Table 5. Proper motions of the HD 114762 AB system measured by different instruments and in different reductions schemes.

Reference	Instrument/reduction	$\mu_{\alpha*}$ (mas yr^{-1})	μ_δ (mas yr^{-1})	$\|\|\Delta\mu_{\rm DR1}\|\|$ (mas yr^{-1})
	HD 114762's system			
Halbwachs et al. (2000)	HIPPARCOS	-582.61 ± 1.13	-1.66 ± 0.96	1.14 ± 0.96
van Leeuwen (2007)	HIPPARCOS-2	-582.87 ± 0.78	-2.48 ± 0.65	2.0 ± 0.7
Gaia Collaboration (2016b,a)	HIPPARCOS + *Gaia* DR1	-582.611 ± 0.041	-0.520 ± 0.039	0.00
Gaia Collaboration (2018)	*Gaia* DR2	-586.29 ± 1.15	2.26 ± 0.40	4.6 ± 1.2
Brandt (2019)	HIPPARCOS + *Gaia* DR2	-582.690 ± 0.030	-0.598 ± 0.028	0.11 ± 0.04
	HD 114762 B			
Faherty et al. (2012)	ANDICAM	-579.62 ± 0.49	-2.1244 ± 0.0018	3.4 ± 0.5

Notes. $\Delta\mu_{\rm DR1}$ measures the difference between the proper motion of the current line with the *Gaia* DR1 proper motion in line 3.

HD 114762 B is responsible for the excess noise observed by *Gaia* in DR1 at the 3σ level.

Table 5 shows the proper motions derived for the HD 114762 AB system using different instruments and reductions. The comparison of the proper motion measured in Faherty et al. (2012) with ANDICAM for HD 114762 B to the proper motion of the HD 114762 system measured in the DR1[2] shows that the relative astrometric motion of B compared to A is about 3.4 mas yr^{-1}. The mass ratio $m_{\rm A}/m_{\rm B} = 0.11$ implies that the relative motion of A compared to the center-of-mass of the AB system as a result of the presence of B should be ~0.34 mas yr^{-1}. Therefore, the existence of HD 114762 B likely affects $\epsilon_{\rm DR1}$ by less than 0.4 mas.

When we conservatively assume that the orbital motion of HD 114762 B contributes $\epsilon_{\rm B} = 0.55$ mas, the remaining excess noise that needs to be explained by the unseen companion HD 114762 Ab is at least $\epsilon_{\rm Ab} = \sqrt{\epsilon^2_{\rm DR1} - \epsilon^2_{\rm B}} = 0.94$ mas. This is still a large significant excess noise. Running GASTON with this new value resulted in a mass for HD 114762 Ab of $108^{+31}_{-26}\,M_{\rm J}$ and an inclination of $6.20^{+1.90}_{-1.30}$ degrees at 1σ. A planetary mass $<13.5\,M_{\rm J}$ is rejected at the 3σ level. The final results for all other fitted parameters are summarized in Table 4.

Interestingly, Halbwachs et al. (2000) fit the astrometric reflex motion of HD 114762 A as a result of HD 114762 Ab on HIPPARCOS data and found a tentative mass for HD 114762 Ab of $0.105 \pm 0.097\,M_\odot$. The central value of this agrees with our findings.

5. Proper motions of the HD 114762 system

We suggested in Sect. 3 that with an orbital period longer than 500 days, HD 114762 B might be compatible with the small ΔQ factor given in Table 3. For a given system, this quantity is calculated by measuring the significance of the proper motion difference between HIPPARCOS and *Gaia* DR1. Table 5 shows, however, that the proper motions of the HD 114762 system found by HIPPARCOS-2 (van Leeuwen 2007) differ from the *Gaia* DR1 proper motions by a factor that is only compatible with zero at 3σ. A $\Delta\mu \sim 2$ mas would better correspond to the orbital reflex motion of HD 114762 A as a result of HD 114762 Ab, as is typically found for the simulated *Gaia* DR1 data in Table 4.

The proper motions found by Halbwachs et al. (2000) using HIPPARCOS measurements account for the orbital reflex motion caused by HD 114762 Ab. They fully agree with this interpretation, given the resulting difference with *Gaia* DR1 of only 1.14 ± 0.96 mas yr^{-1}. On the other hand, this insignificant difference is compatible with the estimated effect of the wide-orbit companion HD 114762 B because we would expect a proper motion of HD 114762 A of about 0.4 mas yr^{-1}.

The difference with DR2 proper motions is even more pronounced, with $\|\Delta\mu_{\rm DR1-DR2}\| = 4.6 \pm 1.2$ mas yr^{-1}. This should be considered with caution, however, because the source HD 114762 in DR2 is duplicated. Many observations (17 of 29 CCD transits) were not taken into account, which explains the large uncertainties on these proper motions.

6. Conclusions

Based on the *Gaia* astrometry that was published in the first data release of the mission (DR1; Gaia Collaboration 2016b,a), we addressed the puzzling question of the true nature of HD 114762 b. With the GASTON method (Kiefer et al. 2019) and the large astrometric excess noise of 1.09 mas measured by *Gaia* for this system, we derived an inclination of $4.87^{+1.11}_{-0.91}$ degree for the orbit of HD 114762 b. This leads to a mass of the companion of $M_{\rm b} = 141^{+35}_{-28}\,M_{\rm J}$ and greater than $68\,M_{\rm J}$ at the 3σ level. This confirms the initial doubts on the planetary nature of the companion, which were based on the $v \sin i$ of the primary star. This had been found to be significantly lower than the expected rotational velocity for a G-type star like this.

We investigated the effect of the presence of the wide-orbit companion HD 114762 B. We found that while it might be responsible for part of the astrometric motion of HD 114762 A, it is likely not the explanation for an excess noise as high as 1.09 mas. When we accounted for this binary component, we found that the mass of HD 114762 Ab would decrease toward the brown dwarf domain, with $M_{\rm b} = 108^{+31}_{-26}\,M_{\rm J}$. A planetary mass $<13.5\,M_{\rm J}$ for this companion is rejected at 3σ.

The companion HD 114762 b has been reported to be a planetary candidate with a mass of at least $11\,M_{\rm J}$, but we showed here that its true mass is significantly higher and does not lie in the planetary domain. The hot Jupiter 51 Peg b (Mayor & Queloz 1995) was thus indeed the first planet that was discovered to orbit another solar-type star. The mass of 51 Peg b is moreover well determined within the planetary domain by the observation of its dayside spectrum (Birkby et al. 2017).

Finally, we showed here that the GASTON method and *Gaia* DR1 astrometric data can be useful for characterizing the mass of RV-detected companions. This will be the subject of a future article (Kiefer et al., in prep.).

[2] Brandt (2018, 2019) published HIPPARCOS-*Gaia* DR2 proper motion, similar to the *Gaia* DR1 proper motions for the TGAS sample. It resulted in small corrections of the DR1 proper motions found for the HD 114762 system, $\Delta\mu_{\rm DR1} = (-0.08, -0.08)$ mas yr^{-1}.

Acknowledgements. I am thankful to the anonymous referee for his help in improving the manuscript and the analysis. I warmly thank Michel Mayor for the fruitful discussions on the present subject. I am also thankful to A. Lecavelier and G. Hébrard for their advices and careful readings of the paper. This work was supported by a fellowship grant from the Centre National d'Etude Spatiale (CNES). This work has made use of data from the European Space Agency (ESA) mission *Gaia* (https://www.cosmos.esa.int/gaia), processed by the *Gaia* Data Processing and Analysis Consortium (DPAC; https://www.cosmos.esa.int/web/gaia/dpac/consortium).

References

Birkby, J. L., de Kok, R. J., Brogi, M., et al. 2017, AJ, 153, 138
Bowler, B. P., Liu, M. C., & Cushing, M. C. 2009, ApJ, 706, 1114
Brandt, T. D. 2018, ApJS, 239, 31
Brandt, T. D. 2019, ApJS, 241, 39
Butler, R. P., Wright, J. T., Marcy, G. W., et al. 2006, ApJ, 646, 505
Cochran, W. D., Hatzes, A. P., & Hancock, T. J. 1991, ApJ, 380, L35
Faherty, J. K., Burgasser, A. J., Walter, F. M., et al. 2012, ApJ, 752, 56
Foreman-Mackey, D., Hogg, D. W., Lang, D., et al. 2013, PASP, 125, 306
Gaia Collaboration (Brown, A. G. A., et al.) 2016a, A&A, 595, A2
Gaia Collaboration (Prusti, T., et al.) 2016b, A&A, 595, A1
Gaia Collaboration (Brown, A. G. A., et al.) 2018, A&A, 616, A1
Halbwachs, J. L., Arenou, F., Mayor, M., et al. 2000, A&A, 355, 581
Hale, A. 1995, PASP, 107, 22
Hébrard, G., Bouchy, F., Pont, F., et al. 2008, A&A, 488, 763
Johnson, M. C., Cochran, W. D., Addison, B. C., et al. 2017, AJ, 154, 137
Kane, S. R., Henry, G. W., Dragomir, D., et al. 2011, ApJ, 735, L41
Kiefer, F., Hébrard, G., Sahlmann, J., et al. 2019, A&A, 631, A125
Latham, D. W., Mazeh, T., Stefanik, R. P., et al. 1989, Nature, 339, 38
Lindegren, L., Lammers, U., Hobbs, D., et al. 2012, A&A, 538, A78
Lindegren, L., Lammers, U., Bastian, U., et al. 2016, A&A, 595, A4
Lindegren, L., Hernández, J., Bombrun, A., et al. 2018, A&A, 616, A2
Lovis, C., & Fischer, D. 2010, Exoplanets (Tucson, AZ: University of Arizona Press), 27
Matsuo, T., Shibai, H., Ootsubo, T., et al. 2007, ApJ, 662, 1282
Mayor, M., & Queloz, D. 1995, Nature, 378, 355
Mazeh, T., Latham, D. W., & Stefanik, R. P. 1996, ApJ, 466, 415
Michalik, D., Lindegren, L., Hobbs, D., et al. 2014, A&A, 571, A85
McCormac, J., Gillen, E., Jackman, J. A. G., et al. 2019, MNRAS, submitted [arXiv:1909.12424]
Mordasini, C., Alibert, Y., Benz, W., et al. 2012, A&A, 541, A97
Nordström, B., Mayor, M., Andersen, J., et al. 2004, A&A, 418, 989
Patience, J., White, R. J., Ghez, A. M., et al. 2002, ApJ, 581, 654
Perryman, M., Hartman, J., Bakos, G. Á., & Lindegren, L. 2014, ApJ, 797, 14
Stassun, K. G., Collins, K. A., & Gaudi, B. S. 2017, AJ, 153, 136
Triaud, A. H. M. J., Collier Cameron, A., Queloz, D., et al. 2010, A&A, 524, A25
van Leeuwen, F. 2007, A&A, 474, 653
Winn, J. N., Noyes, R. W., Holman, M. J., et al. 2005, ApJ, 631, 1215

Appendix A: New developements compared to Kiefer et al. (2019)

A.1. MCMC simulations

In K19, we used a simple bounding of inclinations that are compatible with the excess noise up to a roughly estimated error of ∼10%. Bayesian inference could allow us to deduce at $p = 68.3\%$ the possible lower (upper) limits on the mass of the secondary using many *Gaia* measurement simulations, where inclinations are drawn from a uniform distribution. This has several drawbacks:

- The actual true prior on the inclination is not uniform, but rather follows $p(\theta) = \sin(\theta)\mathrm{d}\theta$ because the unit vector of the edge-on configurations of a system describes a larger solid angle than the face-on configuration.
- It follows that the deduced inclination has to be biased toward 90°. This is especially important in systems for which *Gaia* is only able to give a lower limit constraint on the inclination, and the upper limit is compatible with 90°. The most likely inclination is probably closer to 90° than to the median of the interval.
- Finally, inclinations close to 0° are too poorly sampled from a uniform distribution.

These problems are best addressed with a proper MCMC algorithm. In this study, we used `emcee` (Foreman-Mackey et al. 2013).

A.2. Parameter space and priors

The parameter space is first mapped to $\mathbb{R}^9$ using the following set of relations $\lambda_i = \psi(\rho_i)$:

$$\lambda_\theta = \psi(\theta) = \tan(2\theta - \pi/2)$$
$$\lambda_P = \psi(P) = \ln P$$
$$\lambda_{e_\mathrm{b}} = \psi(e_\mathrm{b}) = \tan(\pi(e_\mathrm{b} - 1/2))$$
$$\lambda_\omega = \psi(\omega) = \tan(\frac{\omega - \pi}{2})$$
$$\lambda_{T_\mathrm{p}} = \psi(T_\mathrm{p}) = T_\mathrm{p}$$
$$\lambda_{M_\mathrm{b}\sin i} = \psi(M_\mathrm{b}\sin i) = \ln M_\mathrm{b}\sin i$$
$$\lambda_{M_\star} = \psi(M_\star) = \ln M_\star$$
$$\lambda_\pi = \psi(\pi) = \ln \pi$$
$$\lambda_{f,\epsilon} = \psi(f_\epsilon) = \ln f_\epsilon$$
$$\lambda_{f,K} = \psi(f_K) = f_K.$$

In addition to the inclination, the prior distributions mostly include Gaussian constraints on all orbital parameters (P, e_b, ω, T_p, $M_\mathrm{b}\sin i$, π, and $M_\star$). The uncertainty on ϵ^2 is estimated based on theoretical calculations developed in Appendix A.3. It might be over- or underestimated. A hyperparameter f_ϵ allows rescaling the uncertainty of ϵ^2 to $f_\epsilon\,\sigma_{\epsilon^2}$. Moreover, given that the Kane et al. (2011) solution for the HD 114762 b Keplerian orbit fit leads to a reduced $\chi^2 = 1.3$, that is, larger than 1, we quadratically add to σ_K a jitter term $\sigma_\mathrm{jitter} = f_K\,\sigma_K$. Finally, the prior on inclinations takes the results of the above discussion into account.

The prior distributions are defined as follows:

$$p(\lambda_\theta) = \frac{1/2}{1+\lambda_\theta^2}\ \sin\left(\arctan(\lambda_\theta)/2 + \pi/4\right)\ \mathrm{d}\lambda_\theta$$

$$p(\lambda_P) = e^{\psi(P)}\ \exp\left(-\frac{(P - P_\mathrm{mes})^2}{2\,\sigma_P^2}\right)\frac{\mathrm{d}\lambda_P}{\sqrt{2\pi\sigma_P^2}}$$

$$p(\lambda_{e_\mathrm{b}}) = \frac{1/\pi}{1+\lambda_{e_\mathrm{b}}^2}\ \exp\left(-\frac{(\arctan(\lambda_{e_\mathrm{b}})/\pi + 1/2 - e_\mathrm{mes})^2}{2\,\sigma_{e_\mathrm{b}}^2}\right)\frac{\mathrm{d}\lambda_{e_\mathrm{b}}}{\sqrt{2\pi\sigma_{e_\mathrm{b}}^2}}$$

$$p(\lambda_\omega) = \frac{2}{1+\lambda_\omega^2}\ \exp\left(-\frac{(2\arctan(\lambda_\omega) + \pi - \omega_\mathrm{mes})^2}{2\,\sigma_\omega^2}\right)\frac{\mathrm{d}\lambda_\omega}{\sqrt{2\pi\sigma_\omega^2}}$$

$$p(\lambda_{T_\mathrm{p}}) = \exp\left(-\frac{(e^{\lambda_{T_\mathrm{p}}} - T_{p,\mathrm{mes}})^2}{2\,\sigma_{T_\mathrm{p}}^2}\right)\frac{\mathrm{d}\lambda_{T_\mathrm{p}}}{\sqrt{2\pi\sigma_{T_\mathrm{p}}^2}}$$

$$p(\lambda_{M_\mathrm{b}\sin i}) = e^{\lambda_{M_\mathrm{b}\sin i}}\ \exp\left(-\frac{(e^{\lambda_{M_\mathrm{b}\sin i}} - M_\mathrm{b}\sin i_\mathrm{mes})^2}{2\,\sigma_{M_\mathrm{b}\sin i}^2}\right)\frac{\mathrm{d}\lambda_{M_\mathrm{b}\sin i}}{\sqrt{2\pi\sigma_{M_\mathrm{b}\sin i}^2}}$$

$$p(\lambda_{M_\star}) = e^{\lambda_{M_\star}}\ \exp\left(-\frac{(e^{\lambda_{M_\star}} - M_{\star,\mathrm{mes}})^2}{2\,\sigma_{M_\star}^2}\right)\frac{\mathrm{d}\lambda_{M_\star}}{\sqrt{2\pi\sigma_{M_\star}^2}}$$

$$p(\lambda_\pi) = e^{\lambda_\pi}\ \exp\left(-\frac{(e^{\lambda_\pi} - \pi_\mathrm{mes})^2}{2\,\sigma_\pi^2}\right)\frac{\mathrm{d}\lambda_\pi}{\sqrt{2\pi\sigma_\pi^2}}$$

$$p(\lambda_{f,\epsilon}) = e^{\lambda_{f,\epsilon}}\ \exp\left(-\frac{(e^{\lambda_{f,\epsilon}} - 1)^2}{2\,\sigma_{f,\epsilon}^2}\right)\frac{\mathrm{d}\lambda_{f,\epsilon}}{\sqrt{2\pi\sigma_{f,\epsilon}^2}}$$

$$p(\lambda_{f,K}) = \frac{\mathrm{d}\lambda_{f,K}}{\sqrt{3}}.$$

For each parameter $\lambda = \psi(\rho)$, the centroid ρ_mes, and associated uncertainties σ_ρ are taken to be those given in Table 2. Exception are the f_ϵ and f_K factors. The prior on f_ϵ is centered around 1 with $\sigma = 0.1$, assuming that the errors on ϵ^2 could be adjusted up to ∼10%. The prior on f_K is taken to be uniform between 0 and $\sqrt{3}$. The upper limit corresponds to a correction for semi-amplitude uncertainties by a factor of 2. The jitter correction cannot be much larger than the semi-amplitude uncertainty, unless the reduced χ^2 of the RV Keplerian fit strongly departs from 1. To derive the orbit of HD 114762 b, Kane et al. (2011) arrived at a reduced χ^2 of 1.3, and thus the jitter term should be on the order of $0.55 \times \sigma_K \sim 2\,\mathrm{m\,s^{-1}}$ in order to obtain $\chi^2_\mathrm{red} = 1$.

A.3. Likelihood and data-point uncertainties

The likelihood includes the weighted squared distance of simulations to two data points: the square of the total excess noise $\epsilon^2_\mathrm{tot,mes}$ (as defined below), and the semi-amplitude of the RVs, K_mes. The log-likelihood up to a constant is expressed as

$$\ln\mathcal{L} \propto \frac{1}{2}\left(\frac{\left(\epsilon^2_\mathrm{tot,simu} - \epsilon^2_\mathrm{tot,mes}\right)^2}{\left(e^{\lambda_{f,\epsilon}}\sigma_{\epsilon^2_\mathrm{tot}}\right)^2} + \frac{(K_\mathrm{simu} - K_\mathrm{mes})^2}{\sigma_K^2 + f_K^2 K^2} + 2\ln\left(e^{\lambda_{f,\epsilon}}\sigma_{\epsilon^2_\mathrm{tot}}\right) + \ln\left(\sigma_K^2 + \sigma^2_\mathrm{jitter}\right)\right). \tag{A.1}$$

For given orbital parameters, the value of the simulated semi-amplitude, K_simu, is calculated using the standard formula (see e.g. Lovis & Fischer 2010),

$$K_\mathrm{simu} = \frac{28.4329\,\mathrm{m/s}}{\sqrt{1-e_\mathrm{b}^2}}\,\frac{M_\mathrm{b}\sin i}{1\,M_\mathrm{J}}\left(\frac{M_\star}{1\,M_\odot}\right)^{-2/3}\left(\frac{P}{1\,\mathrm{yr}}\right)^{-1/3}.$$

The total excess noises $\epsilon^2_{\rm tot,simu}$ and $\epsilon^2_{\rm tot,mes}$ are defined as follows:

$$\epsilon^2_{\rm tot,simu} = \sum_{i=1}^{N_{\rm DR1}} R_i^2/(N_{\rm DR1}-5)$$
$$\epsilon^2_{\rm tot,mes} = \epsilon^2_{\rm DR1} + \sigma^2_{\rm AL},$$

with $\epsilon_{\rm DR1}$ the excess noise published in *Gaia* DR1. Ideally, parameters should be found that lead to residuals R_i that are compatible with $\sum_{i=1}^{N_{\rm DR1}} R_i^2/(N_{\rm DR1}-5) = \epsilon^2_{\rm tot,mes}$ following the definition of the excess noise measured by *Gaia* in Lindegren et al. (2012), for instance.

Using $\epsilon^2_{\rm tot}$ rather than $\epsilon_{\rm DR1}$ as a data point in the MCMC appeared the most natural choice. According to the above formula, $\epsilon^2_{\rm tot}$ is calculated like a χ^2 with $N_{\rm dof} = N_{\rm DR1} - 5$ degrees of freedom (dof); where $N_{\rm DR1}$ is the number of data points and $\nu = 5$ is the number of astrometric parameters that are fit by *Gaia* (Lindegren et al. 2016). To some extent, the purely stochastic part of $\epsilon^2_{\rm tot}$ follows a χ^2 distribution with large $N_{\rm dof}$ (typically 100) and thus an approximate Gaussian distribution. It is therefore quite natural to express errors on the determination of the excess noise directly on $\epsilon^2_{\rm tot}$.

The uncertainty on $\epsilon^2_{\rm tot}$ is the most important term of the likelihood because it scales the posterior distribution of inclinations, and therefore the resulting true mass of the companion. The residuals in the above formula can be expressed as the sum of a non-stochastic term Q_i fixed by the λ parameters and a purely stochastic random variable r_i with assumed Gaussian distribution, $R_i = Q_i(\lambda) + r_i$. The uncertainty on $\epsilon^2_{\rm tot}$ is the square root of its variance V, which can be written as

$$V\left(\frac{\sum_i R_i^2}{N_{\rm DR1}-5}\right) = V\left(\frac{\sum_i Q_i^2}{N_{\rm DR1}-5}\right) + V\left(\frac{\sum_i r_i^2}{N_{\rm DR1}-5}\right) + 4\,V\left(\frac{\sum_i Q_i r_i}{N_{\rm DR1}-5}\right).$$

The first term can be approximated by a Monte Carlo method, measuring the variance of the $\epsilon^2_{\rm tot}$ distribution spanned by N randomly selected series of epochs and scan angle $\{t_i, \phi_i\}$ at a given set of λ parameters. This part is crucial because the exact epochs and scan angles that are selected by *Gaia* are unknown to us. Omitting this term means that too many parameter sets are rejected that are explored with the MCMC, leading to mean acceptance rates as low as 0.10, while it should rather stand about 0.25

$$V\left(\sum Q_i^2/(N_{\rm DR1}-5)\right) \approx {\rm Var}\left(\epsilon^{(i)}_{\rm tot,simu};\ i \in [1,N];\ \lambda s \text{ given}\right).$$

The sum of the two remaining terms is a (mostly) stochastic contribution to the uncertainty on $\epsilon^2_{\rm tot}$,

$$V\left(\frac{\sum_i r_i^2}{N_{\rm DR1}-5}\right) + 4\,V\left(\frac{\sum_i Q_i r_i}{N_{\rm DR1}-5}\right) = \frac{4\sigma^2_{\rm noise}}{N-5}\left(\epsilon^2_{\rm tot,simu} - \frac{\sigma^2_{\rm noise}}{2}\right).$$

This comes on the one hand from the measurement errors of the scanning process on the *Gaia* CCD detector ($\sigma_{\rm AL} \sim 0.4$ mas) and on the other hand from a systematic scatter of diverse origins, such as the imperfect modeling of the spacecraft attitude, with $\sigma_{\rm sys} \sim 0.5$ mas (Lindegren et al. 2016; Kiefer et al. 2019). The total stochastic noise on residuals therefore scales as $\sigma^2_{\rm noise} = \sigma^2_{\rm AL} + \sigma^2_{\rm sys}$.

A.4. Running the MCMC

The MCMC process is run for 200 walkers with a burn-in phase of 600 steps and 10 000 more iterations to derive the posterior distributions on $\{\theta, P, e_{\rm b}, \omega, T_{\rm p}, M_{\rm b}\sin i, M_\star, \pi, f_\epsilon,$ and $f_K\}$. The initial starting point for inclination θ is determined from a straightforward minimization of the χ^2 using a grid of possible inclinations ranging from 0 to 90°. The average autocorrelation length converges to 180 steps. The number of iterations required to calculate the posterior distributions are therefore more than 50 times this length, as is usually recommended. The mean acceptance rate of the MCMC runs stands about 0.25, which is a typical value expected for parameter spaces with nine dimensions. The posterior distribution of the fit parameters in our case is shown in Fig. A.1, and the results are presented in Table 4. For the jitter correction for the RV semi-amplitude uncertainty, we report the posterior of $\sigma_{\rm jitter}$ in m s^{-1}, rather than the dimensionless f_K.

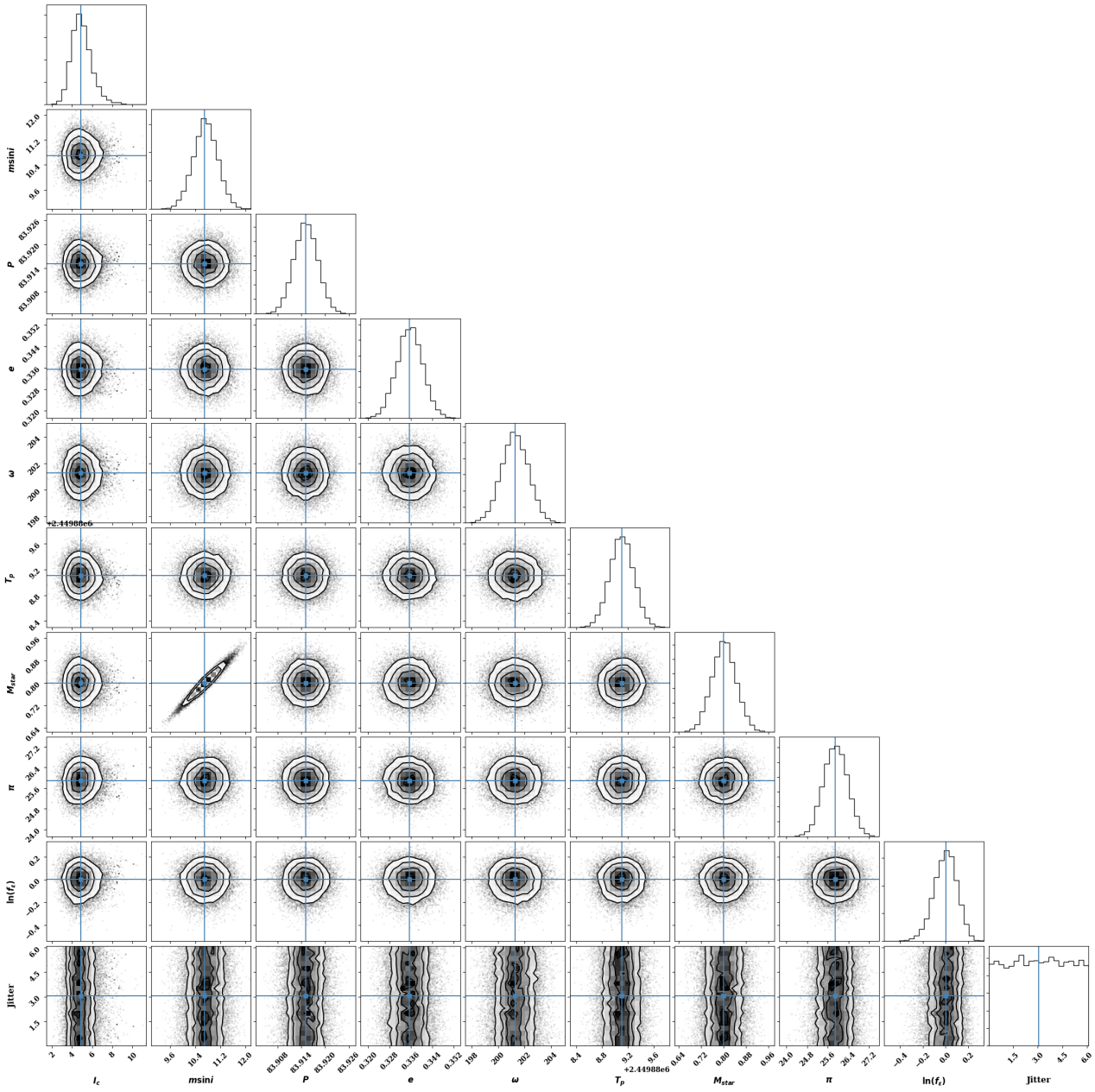

Fig. A.1. Posterior distribution and correlations of the parameters presented in Table 4, neglecting the effect of HD 114762 B. The RV parameters are constrained based on data from Kane et al. (2011) and on the parallax from *Gaia* DR1.